

# STRUCTURAL BEHAVIOR OF ENGINEERING WOOD ENCASED CONCRETE-STEEL COMPOSITE COLUMNS

FAUZAN\*<sup>1</sup>, Hiroshi KURAMOTO\*<sup>2</sup>, Yutaka SHIBAYAMA\*<sup>3</sup> and Tetsurou YAMAMOTO\*<sup>3</sup>

**ABSTRACT:** This paper presents the results from a feasibility study on the structural behavior of an engineering wood encased concrete-steel (EWECS) composite column and a concrete encased steel (CES) composite column without cover concrete. The two columns were tested under constant axial load and lateral load reversals. The main key parameter was the presence of woody shell. From test results, the EWECS column indicated to have a stable spindle-shape hysteresis characteristic, shear force-story drift angle relationship, and enhanced flexural capacity due to the existence of woody shell.

**KEYWORDS:** Concrete-encased steel composite column, woody shell, cyclic load, hysteresis loop, curvature

## 1. INTRODUCTION

Steel reinforced concrete (SRC) structures are typical composite structural systems consisting of steel and reinforced concrete (RC), which have excellent earthquake resistance with high capacities and deformability. However, the design process and construction work are more complicated than those for RC structures and steel structures. In order to solve these problems, concrete encased steel (CES) structures have been proposed by the authors [1]. The experimental studies of CES columns using normal concrete, high performance fiber reinforced cementitious composites (HPFRCC) and fiber reinforced concrete (FRC) had been already conducted [1-3], and as to basic structural performance it was found that the hysteretic characteristics of the CES columns were almost the same as those of SRC columns.

In order to realize the simplification of construction works and the cost reduction in structural materials, the authors propose CES columns using timber material, which consists of CES core and woody shell panels, hereafter referred to as engineering wood encased concrete-steel (EWECS) composite columns, as shown in Fig 1c.

EWECS columns have some advantages over SRC columns because the woody shell panels serve as formwork and give a natural beauty finish of the columns, thus reducing its construction costs. Additionally, the presence of woody shell makes the weight of the columns small. Compared with timber structures, on the other hand, the EWECS columns can be expected to have higher structural performance and fire resistance.

This paper presents the results of an experimental study on the structural performance of an EWECS composite column subjected to constant axial load and lateral load reversals, which is compared with the performance of a CES composite column without cover concrete.

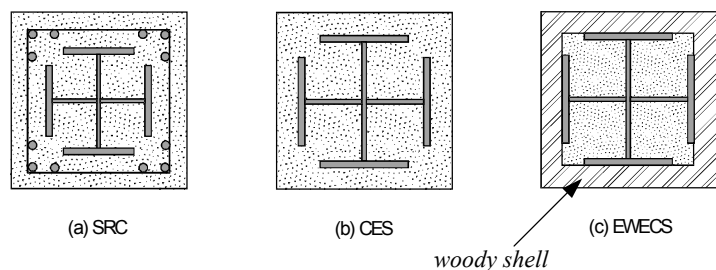


Fig. 1 Types of composite columns

\*1 Department of Architecture and Civil Engineering, Toyohashi University of Technology, Graduate student, MSc.Eng., Member of JCI

\*2 Department of Architecture and Civil Engineering, Toyohashi University of Technology, Associate Professor, Dr., Eng., Member of JCI

\*3 Department of Architecture and Civil Engineering, Toyohashi University of Technology, Graduate student, Member of JCI

## 2. EXPERIMENTAL PROGRAM

### 2.1 SPECIMENS AND MATERIALS USED

Two composite columns, specimens WCS and CS, of which the scale is about two-fifth, were prepared. The dimensions and details of the specimens are shown in Fig. 2 and Table 1. All specimens had a column with 1600 mm height. The column section of the specimen WCS was 400 mm square, while that of the specimen CS was 300 mm square. The specimen WCS was covered by woody shell with a thickness of 45 mm, while the core section was the same as that of the specimen CS. Steel encased in each column had a cross shape section combining two H-section steels of 300x150x 6.5x9 mm. The mechanical properties of the steel and the woody shell are listed in Tables 2 and 3, respectively. Normal concrete of 35 MPa was used for the both specimens. The mix proportions and mechanical properties of the concrete are given in Table 4.

In the specimen WCS, the casting of concrete was carried out after assembling and constructing the woody shell panels to the column by using super wood glue, because the panels serve as mold forms for concrete placement.

The ultimate flexural strengths for each column listed in Table 5 were calculated by fiber section analysis in which the modified Kent and Park model [4] and the perfect elasto-plastic model were used for the stress-strain relationships of concrete and steel, respectively. On the other hand, the original Kent and Park model [5] was used for stress-strain relationship of woody shell.

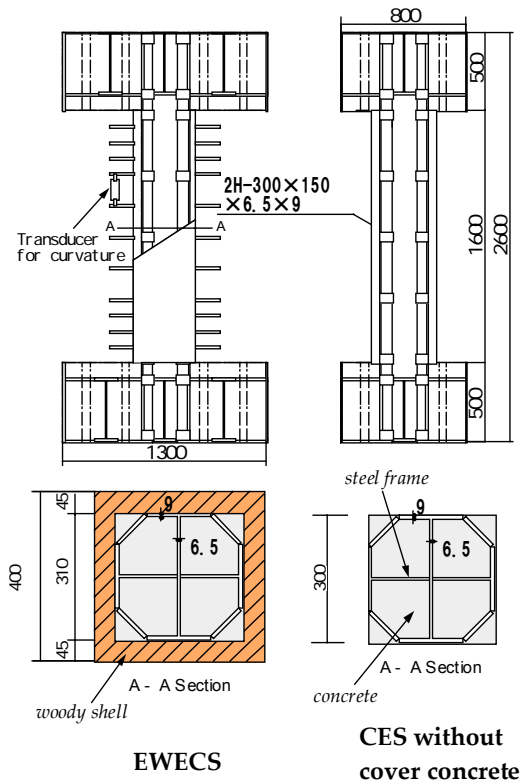


Fig. 2 Test specimen

Table 1 Test program

Specimen	WCS	CS
Column Type	EWECS	CES without cover concrete
Woody Shell Thickness (mm)	45	-
Concrete	Normal Concrete	
Steel	Built-in steel (mm)	WH-300 x 150 x 6.5 x 9
	Tie plate (mm)	PL-9
Column Height: h (mm)	1600	
Cross section : b x D (mm)	400 x 400	300 x 300
Axial Compression	N (kN)	770
	$N/(b \cdot D \cdot \sigma_B)$	0.14

$\sigma_B$ , uniaxial compressive strength of concrete

Table 2 Mechanical properties of steel

Steel	Elastic Modulus $E_s$ (GPa)	Yield Stress $\sigma_y$ (MPa)	Notes
WH-300x150x6.5x9	206.3	412.5	Flange
	226.5	453	Web
PL-9	206.3	412.5	Tie Plate

Table 3 Mechanical properties of woody shell

Woody Shell (mm)	Wood type	<sup>a</sup> Comp. Strength $\sigma_w$ (MPa)	Elastic Modulus $E_s$ (GPa)
40x160x45	Glue laminated pine wood	36.5	10.5

<sup>a</sup> the direction is parallel to axis of grain. The strengths in other directions (perpendicular and tangential to grain) were not measured in this study.

Table 5 Calculated strength

Specimen	WCS	CS
Ultimate flexural strength: $Q_{mcal}$ (kN)	671	508

Table 4 Mix proportions and mechanical properties of concrete

W/C (%)	S/(S+G) (%)	Slump (cm)	Unit weight (kg/m <sup>3</sup> )					Comp. Strength MPa
			Water (W)	Cement (C)	Sand (S)	Gravel (G)	Admixture (A)	
53.5	49.2	21	192	359	836	878	3.59	35.3

## 2.2 TEST SETUP AND LOADING PROCEDURES

The specimens were loaded lateral cyclic shear forces by a horizontal hydraulic jack and a constant axial compression of 770 kN by two vertical jacks, as shown in Photo 1. The applied axial force ratio,  $N/(b.D.\sigma_B)$ , for the specimen CS was 0.25, while that for the specimen WCS was smaller due to the presence of woody shell. The ratio considering the cross section of woody shell for the specimen WCS was about 0.14.

The loads were applied through a steel frame attached at the top of a column that was fixed to the base. The two vertical jacks applying the constant axial compression were also used to keep the column top beam parallel to the bottom beam, so that the column would be subjected to anti-symmetric moments.

The incremental loading cycles were controlled by story drift angles,  $R$ , which was given by the ratio of lateral displacements to the column height,  $\delta/h$ . In this experiment, the specimens were cyclically loaded twice for  $R$  of 0.005, 0.01, 0.015, 0.02, 0.03 and 0.04 radians, and once for that of 0.05 radian, respectively.



**Photo 1 Loading apparatus**

## 3. EXPERIMENTAL RESULTS AND DISCUSSIONS

### 3.1 HYSTERESIS CHARACTERISTICS AND FAILURE MODES

Shear versus story drift angle relationships of the both specimens are compared in Fig. 3. In the figure, the solid and dotted lines represent the measured hysteresis loops of the specimens WCS and CS, respectively. The yield and maximum strengths and the corresponding story drift angles for each specimen are listed in Table 6. The yielding of each specimen was assumed when the first yielding of steel flange at the top and bottom of the columns was observed, which corresponds to a triangle mark on the shear versus story drift angle response (see Fig.3). Failure patterns of the specimen WCS at  $R$  of 0.03 and 0.05 radians are shown in Photo 2. In this test, the damage of the specimen WCS was only observed at the column faces due to the limitation of equipment to observe the damage in the column core.

The both specimens showed ductile and stable spindle-shape hysteresis loops without significant capacity reduction until the maximum story drift,  $R$  of 0.05 radian.

In the specimen CS, flexural cracks occurred at  $R$  of 0.005 radian at both the top and bottom of the column. Subsequently, the cracks extended at the corners of the column with an increase of the story drift angle. Although the cracks propagated, the shear force slightly increased with the increase of the story drift angle. At a shear force of about 370 kN and a story drift,  $R$  of 0.0088 radian, the column reached the first yielding, and the maximum strength of 513 kN was reached at  $R$  of 0.05 radian.

Compared with the specimen CS, the specimen WCS resulted in the increase of maximum flexural strength and ductility. Up to a story drift,  $R$  of 0.03 radian, no damage was observed for the column faces. At this stage, however, sink and uplift of woody shell occurred at the two opposite sides of both the top and bottom of the column, as shown in Photo 2. The first yielding of steel flange occurred at  $R$  of 0.0076 radian and a shear force of 350.5 kN, and the maximum flexural strength of 573 kN was reached at  $R$  of 0.04 radian. The woody shell then buckled outward, and finally the cracks of the woody shell occurred at the corners of the column at  $R$  of 0.05 radian.

As revealed by comparing the hysteresis loops and damage situations of the both specimens, the woody shell contributed to improve the structural performance and reduce the damage in composite columns. In addition, because only the compressive strength of woody shell with  $Y$  direction (parallel to grain) was measured, the effect of strength in different directions on hysteresis characteristic was not discussed in this paper.

The comparisons between the measured and the predicted flexural strength of the specimens are also shown in Fig. 3. The measured maximum flexural strength of the specimen CS fairly agreed with the

calculated flexural strength. For the specimen WCS, on the other hand, the calculated flexural strength was 1.17 times larger than the measured maximum flexural strength. The effect of sink and uplift, shown in photo 2a, may have contributed to the decrease of flexural capacity obtained from experimental results. This means that the assumption of plane sections remain plane after loading in flexural theory is only valid until sink and uplift occur at R of 0.03 radian.

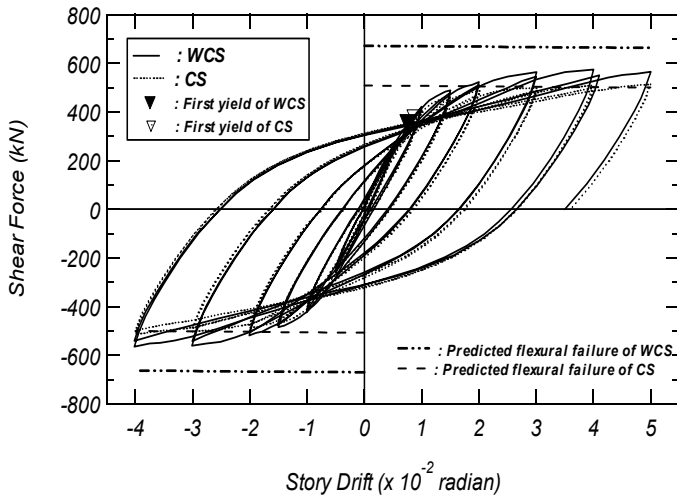


Fig. 3 Shear force - story drift angle relationship

Table 6 Measured strength

Specimen	at Yielding		at the Max. Capacity	
	Q <sub>v</sub> (kN)	R <sub>v</sub> (rad.)	Q <sub>max</sub> (kN)	R <sub>max</sub> (rad.)
CS	370	0.0088	513	0.05
WCS	350.5	0.0076	573	0.04

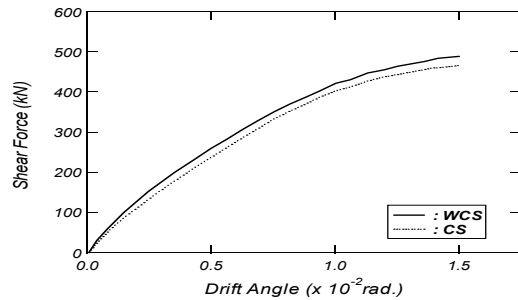


Fig. 4 Initial stiffness



(a) Sink and uplift of woody shell at R = 0.03 rad.

(b) Final cracks of woody shell at R = 0.05 rad.

**Photo 2 Failure patterns of EW ECS column after loading**

Figure 4 shows the comparison of initial stiffness for the both specimens. It was found that the initial stiffness of the specimen WCS was slightly higher than that of the specimen CS, due to the existence of woody shell. This indicated that the initial structural performance of CES column can be improved by arranging woody shell.

**3.2 AXIAL DEFORMATION**

Figure 5 shows the comparison of the longitudinal elongation versus drift angle relationships of the both specimens. The longitudinal elongations of the specimens were recorded from two vertical transducers installed at the midheight of the column, as shown in Fig. 6. The solid and dotted lines represent the development of elongations for the specimens WCS and CS, respectively. As shown in the figure, the longitudinal elongations of the both specimens were symmetrical to each cyclic at positive and negative story drift angles. On the other hand, the slope of incremental elongation of the specimen WCS for each cycle was bigger than that of the specimen CS. The reason for this was that the presence of woody shell in the specimen WCS contributed to enhance the moment capacity and stiffness, which resulted in reducing axial force at the compression area and eventually lead to the increase of the elongation. In this test, the contribution of woody shell in improving the moment capacity and stiffness was only effective until sink and up lift occur at R of 0.03 radian.

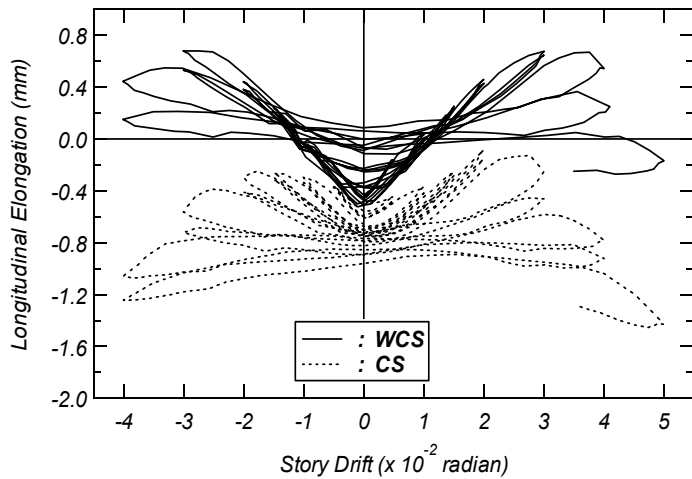


**Fig. 5 Axial deformation**

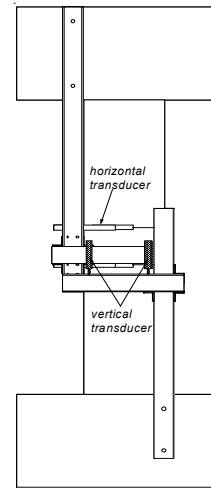


**Fig. 6 Setup transducers**

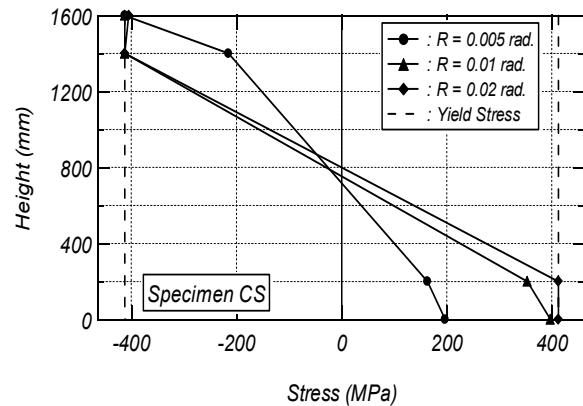
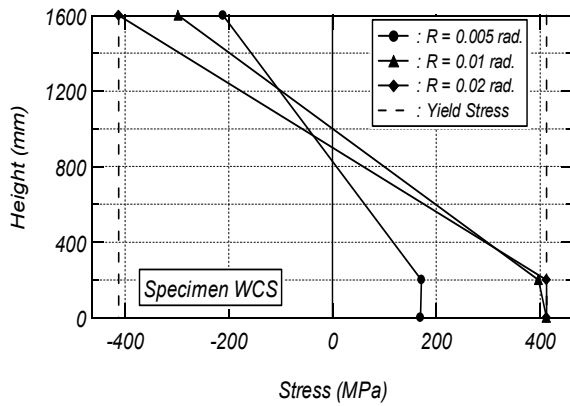


**Fig. 7 Steel stress distribution**

From the figure, it was found that the maximum elongation of 0.7 mm was reached at R of 0.04 radian for the specimen WCS, while in the specimen CS, the maximum elongation of - 0.2 mm was reached at R of 0.03 radian.

### 3.3 STRESS DISTRIBUTION OF ENCASED STEEL

Figure 7 shows stress distributions of encased steel along the column height at R of 0.005, 0.01 and 0.02 radians for the both specimens, which are calculated using the strains from gages installed on the steel flanges. From the figure, it can be seen that the stress distributions in the specimen WCS were different from those of the specimen CS. For the specimen WCS, the stresses in both compression and tension zones at R of 0.005 radian have almost the same level with opposite sign. The first yielding of the specimen occurred in tension zone at R of 0.01 radian. For the specimen CS, on the other hand, the first yielding of the steel flange occurred in compression zone at R of 0.005 radian with a stress of about 200 MPa in tension zone. The higher tensile stress in the specimen WCS at R of 0.01 radian was mainly caused by the reduction of axial force in the compression area due to the existence of woody shell.

However, the same behavior of stress distribution for both specimens was observed at R of 0.02 radian. At this stage, the yielding of the steel flanges was reached in both compression and tension zones.

### 3.4 CURVATURE DISTRIBUTION

Figure 8 shows the curvature distributions along the column height at R of 0.005, 0.01 and 0.015 radians for the both specimens. The values were obtained from transducers installed on the two opposite sides along the column height, as shown in Fig. 2. As seen in the Fig. 8, the curvature distributions of the specimen WCS were almost the same as those of the specimen CS. The highest curvature was found in the

top and bottom of the column for the both specimens. At R of 0.01 and 0.015 radians, however, the maximum curvatures of the specimen WCS were 1.25 times larger than the specimen CS, because higher tensile stress occurred in tension zone at the top and bottom of the column for the specimen WCS.

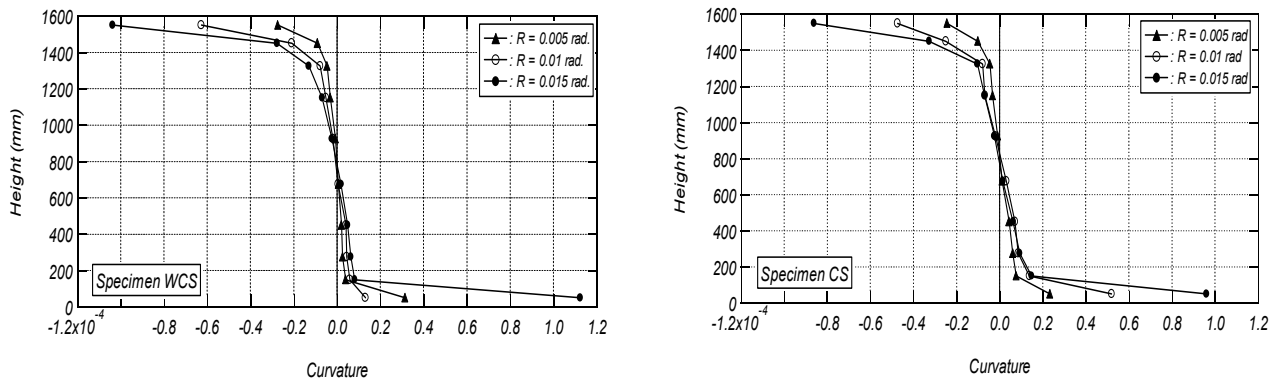


**Fig. 8 Curvature distribution**

#### 4. CONCLUSIONS

Based on the experimental study presented here, the following conclusions can be drawn:

- The EW ECS column has a stable spindle-shape hysteresis characteristic with little damage on the column faces even at a large story drift, R of 0.05 radian.
- The woody shell in the EW ECS column contributes to enhance the strength and ductility, as well as to improve the initial stiffness.
- The woody shell is an effective material for composite column cover, not only to increase the structural performance, but also to simplify the construction works, because it also serves as formwork for concrete placement.
- It was proved that EW ECS column has excellent structural performance, thus, it is considered to be possible to make the EW ECS structural system practical.

#### ACKNOWLEDGEMENT

The authors would like to express their gratitude to the technical staffs of Fujimi Koken Eng. Co., Ltd. for their help and contributions during the casting of concrete for the both specimens.

#### REFERENCES

1. Kuramoto, H., Takahashi, H. and Maeda, M., "Feasibility Study on Structural Performance of Concrete Encased Steel Columns using High Performance Fiber Reinforced Cementitious Composites," Summaries of Technical Papers of Annual Meeting, AIJ, Vol.C-1, 2000, pp. 1085 – 1088 (in Japanese).
2. Adachi, T., Kuramoto, H. and Kawasaki, K., "Experimental Study on Structural Performance of Composite Columns Using FRC," Proceeding of the Japan Concrete Institute, Vol.24, No.2, 2002, pp. 271-276 (in Japanese).
3. Kuramoto, H., Adachi, T. and Kawasaki, K., "Behavior of Concrete Encased Steel Composite Columns Using FRC," Proceedings of Workshop on Smart Structural Systems Organized for US-Japan Cooperative Research Programs on Smart Structural Systems (Auto-Adaptive Media) and Urban Earthquake Disaster Mitigation, Tsukuba, Japan, 2002, pp. 13-26.
4. Park, R., Priestley, M.J.N. and Gill, W.D., "Ductility of Square-Confined Concrete Column," Proceedings of ASCE, Vol.108, No. ST4, 1982, pp. 929 –950.
5. Kent, D.C. and Park, R., "Flexural Members with Confined Concrete," Proceedings of ASCE, Vol.97, No. ST7, 1971, pp. 1969-1990.